ADAPTIVE EQUALISATION FOR CONTINUOUS ACTIVE SONAR?

Konstantinos Pelekanakis, Jeffrey R. Bates, and Alessandra Tesei

Science and Technology Organization - Centre for Maritime Research and Experimentation, La Spezia, SP, ITALY

Contact: Konstantinos Pelekanakis, STO – CMRE 400 Viale San Bartolomeo, 19126 La Spezia (SP), Tel: +39 0187 527 283, email: konstantinos.pelekanakis@cmre.nato.int

Abstract: *Underwater acoustic environments exhibit long and time-varying multipath propagation conditions that severely limit the spatio-temporal coherence of any continuous active sonar (CAS) pulse. Due to this issue, traditional matched filter processing at the receiver does not always achieve the desired processing gains leading to poor target tracking. Hence, a major effort in the field of active sonar is steered towards the design of novel receivers that emphasize on efficient Doppler target tracking while maintaining good range resolution. This paper represents the first attempt to process the target's echoes based on an adaptive decision-feedback equaliser (DFE), a well-known technique applied in underwater acoustic communications. The performance of the proposed signal is tested through a simple experimental setup during a sea trial off the coast of Portugal in 2016. The transmitted binary phase shift keying (BPSK) signal occupied the 1500 - 2500 Hz band and lasted for 7.7 seconds. Our results demonstrate a high-precision Doppler measurement with an update rate of 1 ms for a target moving at 6 knots.*

Keywords: *Underwater acoustic communications, active SONAR, target detection, decision feedback equaliser (DFE), delay spread, Doppler spread.*

1. INTRODUCTION

In typical active SONAR systems, the process of localising a target is performed by transmitting a known signal and then correlating it with returned echoes arriving at specific angles. Recent advances in transducer technology enable Continuous Active SONAR (CAS) systems that allow duty cycles up to 100%. As a result, CAS systems can perform more frequent signal correlations, which could potentially lower the data association error inherent to Pulse Active Sonar (PAS) systems [1].

Linear Frequency Modulated (LFM) broadband signals, conventionally used in PAS, have been tailored to CAS with a significant increase of time-bandwidth product [2]. Theoretically, improved detectability in both noise-limited and reverberation-limited environments is possible, however, the anticipated processing gain can drop significantly when the channel exhibits low spatio-temporal coherence. Understanding the impact of channel coherence on CAS LFM signals is a major research activity nowadays [2]-[5].

Another research activity related to CAS is the adoption of communications waveforms, such as binary phase shift keying (BPSK). In [6], the authors sequentially combine a BPSK with an LFM to improve performance in channel-induced Doppler perturbations, yet, only computer simulations were shown. A comparison between LFM signals and BPSK signals in terms of matched filter processing gains has been illustrated in [7]. The results indicate that the ambiguity function is not adequate to explain the waveform's processing gain for different time-bandwidth products under different channel conditions.

In this work, we depart from the conventional matched filtering signal processing technique and propose to tailor advanced signal equalisation techniques (typically used in underwater acoustic communications [8]) for CAS systems. In particular, we analyse a 1000-bps BPSK signal by using data from the Rapid Environmental Picture Atlantic (REP-Atlantic). Our decision-feedback equaliser (DFE) receiver achieves reliable delay/Doppler estimates for both strong and weak echoes moving at 6 knots. The key result here is that the Doppler measurement update rate of the echo is as fast as the bit rate of the transmitted message.

2. PROPOSED SYSTEM

We consider a SONAR waveform that is based on binary phase-shift keying (BPSK) modulation. Let us assume that N bits are produced from a pseudo-random sequence generator. The N-bit sequence is mapped onto a symbol sequence $\{d_n\}_{n=1}^{N} \in \{-1,1\}$ and the symbols are pulse-shaped via a raised cosine filter with roll-off factor $\alpha \in [0,1]$ at a rate of $1/T$, T being the symbol duration. Note that any filter that yields the zero inter-symbol interference (ISI) property is suitable for our purposes [9]. The baseband signal is modulated onto a carrier f_c and the passband transmitted signal can be represented as

$$x(t) = Re\left\{\sum_{n=1}^{N} d_n g(t - nT) e^{j2\pi f_c t}\right\}, \quad (1)$$

where $g(t)$ denotes the raised cosine filter response. The bandwidth of $x(t)$ is $W = (1 + \alpha)/T$ centered at f_c. Note also that the time-bandwidth product of the signal is approximately N.

Let us now assume that the CAS receiver uses an array of hydrophones steered at a specific angle (or beam) and senses the returned echoes. The end goal of the receiver is to classify whether the observed echoes belong to the target or not. In this preliminary work, we present the receiver structure that potentially feeds the echo classifier with the required target delay/Doppler information. Before we present the receiver structure, we need to put a channel model into perspective. We stress here that the channel model is independent of the type of array used.

Within the considered angle window, the returned echoes undergo both time and Doppler spreading due to time-varying multipath propagation. Here, we model physical phenomena that vary within few seconds or less and hence, comparable to the signal duration. For instance, the effect of sea surface waves onto the received signal is one of them. Transmitter/receiver/target mobility contributes to additional time-variability of the received signal, typically at shorter time scales than channel fluctuations.

Denoting each echo (or multipath) as k, we assume that each multipath has its own time-varying gain $s_k(t)$ and time-varying delay $\tau_k(t)$. For mathematical tractability, we assume that the time-varying delay can be approximated by a first-order polynomial $\tau_k(t) = \tau_k - \beta_k t$, where $\beta_k = u_k/c$, u_k being the radial velocity of the k path and c denoting the speed of sound. Hence, the channel impulse response $h(t,\tau)$ can be expressed as

$$h(t,\tau) = \sum_{k=1}^{K} s_k(t)\delta(\tau - \tau_k + \beta_k t)\ , \tag{2}$$

where $\delta()$ denotes the dirac function. Then, the interaction of the transmitted signal in eq. (1) with the channel response in eq. (2) can be represented via a time-varying convolution sum:

$$y(t) = \int h(t,\tau)x(t-\tau)d\tau + w(t) = \sum_{k=1}^{K} s_k(t)x(t(1+\beta_k) - \tau_k) + w(t), \tag{3}$$

where $w(t)$ denotes the additive ambient noise. Note that when $\beta_k > 0$ the received path experiences a time dilation and when $\beta_k < 0$ the received path experiences a time compression.

The receiver architecture is seen in Fig. 2. The purpose of the wideband beamformer is to scan at different beam angles and sense the incoming signal. Any echoes arriving at the steering angle will experience an SNR increase. The resulting output is processed by an adaptive DFE with the aim to detect each bit sequentially. The DFE performs the following actions:

Adaptive resampling

During the reception of the n^{th} bit, and assuming that the relative motion between the target and receiver is significant, the received signal is time-scaled (compressed or dilated) with respect to the transmitted signal. To reduce the receiver computational complexity, we further assume that all observable echoes exhibit the same time-scale, i.e., $\beta_k = \beta$ for all k. In practice, this is true for certain littoral environments where the range is much greater than the ocean depth and so the channel geometry makes the observe echoes to arrive at (almost) the same angle. To compensate for the time scale β of the n^{th} bit, denoted by $\beta(n)$, we adapt the sampling rate of the received signal with a linear interpolation filter. Prior to interpolation, a first-order phase-locked loop (PLL) estimates the time (or Doppler) scale by processing the phase rotations of all previously received bits. The whole process yields linear computational complexity with respect to the number of parameters involved.

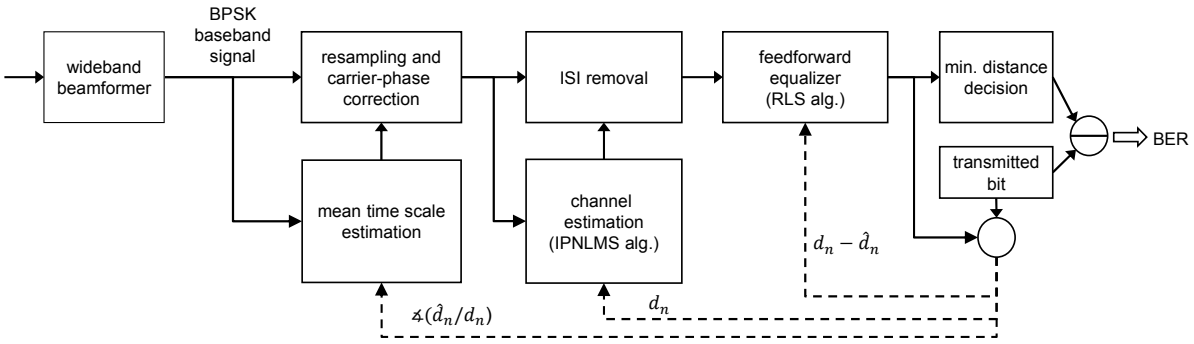

Fig. 1: receiver block diagram.

Adaptive channel estimation and ISI cancelation

After compensating for $\beta(n)$, the transmitted signal consisting of the latest L bits (L denotes the channel multipath delay in terms of number of bits) is used to produce a snapshot of the channel impulse response $h(t,\tau)$ during the n^{th} bit reception. The improved-proportionate normalized least mean squares (IPNLMS) algorithm is used for channel estimation [8]. This algorithm exhibits fast channel tracking by exploiting the sparse multipath structure of the acoustic link. In addition, it offers low memory requirements and linear computational complexity with respect to the number of channel coefficients. Knowing the channel response and the L previously transmitted bits, the ISI is synthesized and subtracted from the received signal.

Adaptive equalisation

The purpose of this part of the receiver is to estimate the n^{th} bit by exploiting the multipath propagation diversity, namely, the receiver coherently combines all echoes that are related to the n^{th} bit for performance improvement. To this end, the received signal is filtered by a linear transversal equaliser to produce $\hat{d}_n$, the complex estimate of the n^{th} transmitted bit. The exponentially-weighted recursive least squares (RLS) algorithm is used to adapt the equaliser coefficients such that the $E\left[\left|d_n - \hat{d}_n\right|^2\right]$ is minimized. The RLS algorithm has quadratic computational complexity with respect to the number of the equaliser taps. The processing gain of the equaliser is measured by the output SNR defined as [9]:

$$SNR_{out} = 10\log_{10}\frac{\sum_{n=1}^{N}|d_n|^2}{\sum_{n=1}^{N}|d_n-\hat{d}_n|^2} \ . \tag{4}$$

Finally, each $\hat{d}_n$ is quantized to the closest ±1 value by measuring their respective Euclidean distances and so a BER estimate is obtained.

3. EXPERIMENTAL RESULTS

The effectiveness of our receiver in terms of estimating the target delay/Doppler is investigated with real data recorded during the Rapid Environmental Picture Atlantic (REP-Atlantic) trial that took place in July, 2016, off the coast of Portugal. On July 11$^{\text{th}}$, 2016, the NRV ALLIANCE towed a sonar source, an echo repeater (acting as an artificial target), and a

64-element linear array (with inter-element spacing of 0.18 m) at approximate depths 70 m, 60 m, and 79 m, respectively.

The sound speed profile was measured at 06:16 UTC by using a *Sea-bird Electronics 9plus* conductivity, temperature, and depth (CTD) sensor and is shown in Fig. 2(a). Note that the sound speed profile is downward refracting, however, both the receiver and echo repeater were below the major thermocline, which ends at about 60 m. At 13:33 UTC, the sea conditions were at sea state 4, with waves coming from the north-west. A dominant wave power spectral density of approximately 6 m^2/Hz at 0.09 Hz was measured by *a Datawell oceanographic instruments MKIII* wave rider.

Between 13:52 and 14:10 UTC, the source concurrently transmitted the proposed BPSK signal and an LFM signal over two distinct bands. The BPSK occupied the 1.3-2.5 kHz band while the LFM occupied the 2.5-3.7 kHz band. The source level was set to 196 dB re 1 µPa @ 1 m. Both signals lasted for 7.7 s and the ping repetition interval was set to 24 s. During the run the NRV ALLIANCE sailed northwest at a speed of 3.5 knots. Fig. 2(b) shows the received spectrogram. The source signal followed by echo repeater signal can be clearly seen. Our purpose is to use the BPSK signal to measure the delay and Doppler of the target. The LFM is used separately to validate our contact acquisition but is not necessary in a realistic system.

As a first step, the hydrophone data is beamformed into 64 cosine spaced beams and matched filtered with a replica of the transmitted LFM. The whole processing is performed in the frequency-domain and Fig. 2(c) shows the output. The red cross signs show potential targets distributed in the delay-angle space. Fig. 2(d) shows the output of the time-domain beamformer after using the BPSK signal. The correspondence between Fig. 2(c) and Fig. 2(d) is clear. We see that the source signal arrives at about 3 degrees while the signal from the echo repeater arrives at about 137 degrees. These numbers agree with the experimental setup, i.e., the source was placed in front of the towing point of the array (endfire) while the echo repeater was placed closer to the trailing edge of the array. Also note that the received power level coming from the source is about 40 dB higher than that of the echo repeater.

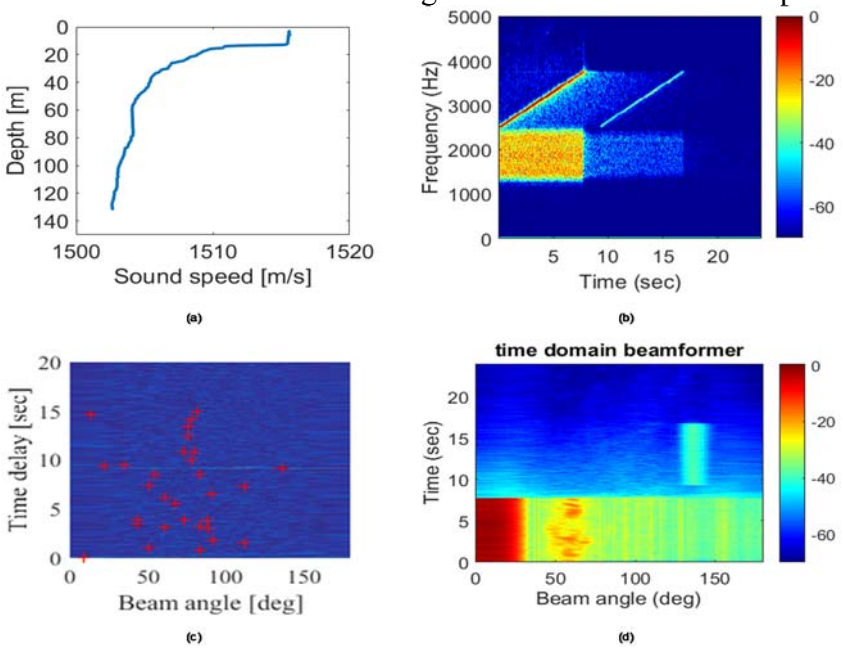

Fig. 2. (a) Measured sound speed profile. (b) Received signal spectrogram. (c) Output of the frequency domain beamformer and matched filter based on the LFM signal. (d) Output of the time domain beamformer based on the BPSK signal.

Our data processing showed that the received BPSK signal was not significantly distorted by ship motion. This happened because of the specific experimental setup, i.e., both transmitters and the array were towed by the same ship and hence, the geometry didn't allow for significant Doppler distortions. To make our results more appealing to the readership and also provide ground-truth, we added an artificial time scale into the received data by resampling. Hereafter, we assume that the target moves away from the receiver at a speed of -3 m/s (≅ 6 knots). This kind of motion makes the receive signal to expand with a the time scale of $\beta = -3/1510 \cong -0.002$.

We now report on the performance of the receiver. We show results for echoes in high and low SNR situations. High SNR is not expected in real-life scenarios; however, better validation of our receiver outputs is possible since any parameter estimation is more reliable. The low SNR provides useful insight about how the receiver would perform in real-life. Below, the contacts are provided by the LFM processor.

Fig. 3 shows the demodulation results when the array is steered towards the echo repeater (angle=137º, delay=9.1 s). The input SNR after beamforming is 26 dB. Fig. 3(a) shows the time evolution of the channel impulse response after motion compensation. The snapshots are generated at the bit rate. The 0 ms delay corresponds to the direct arrival between the echo repeater and the array. We note that overall multipath spread is about 300 ms. In contrast to Fig. 3(a), Fig. 3(b) shows the output of the channel estimator without motion compensation. In this case, the channel estimates are poor due to lack of synchronization and as a result, no bit recovery is possible. Fig. 3(c) shows the average BER estimation as a function of time when the receiver compensates for motion. Note that the BER drops to zero only after 450 ms. This is expected as the receiver needs time to adapt to the channel response and any motion variations. A similar trend is observed for SNR_{out} in Fig. 3(d). Initially, SNR_{out} is close to zero and as the receiver adapts to the channel variations, SNR_{out} reaches eventually 14 dB. Fig. 3(e) shows the estimated mean time (or Doppler) scale, β, of the received signal. Clearly, our receiver estimates the true value with good accuracy.

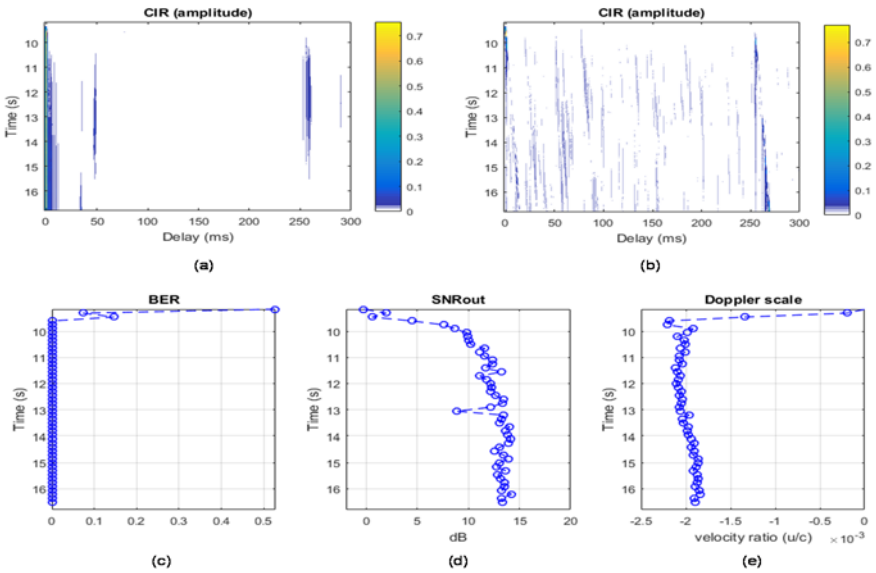

Fig. 3. (a) Channel impulse response after motion compensation. The x-axis shows multipath delay, the y-axis shows absolute time and the z-axis shows the channel amplitude in linear scale. (b) Channel impulse response when zero Doppler is assumed. (c) SNR_{out} vs. time. (d) Mean BER vs. time. (e) Mean Doppler scale vs. time. The averaging interval is set to 150 ms for (c), (d) and (e).

Fig. 4 shows the demodulation results when the array is steered at 75º. At this angle, the receiver senses an echo that involves a surface interaction and arrives at a delay of 12.742 s. The input SNR after beamforming is 11 dB. Fig. 4(a), (b), (c), (d) and (e), illustrate the behaviour of our receiver when the signal delay is 12.730 s, 12.736s, 12.742 s, 12.748s and 12.754 s, respectively. Note that due to channel fading, the target reflects only 4 out of 7.7 s of the signal. Our results show that the receiver is very sensitive with respect to the true delay since high BER (close to 0.5) and low SNR_{out} (close to 0 dB) are measured even for delay offsets of ± 6 ms. Moreover, the Doppler scale estimation is very poor. On the contrary, when the receiver is perfectly synchronized, we observe low BER and high SNR during the periods of sufficient signal level. Moreover, the receiver estimates the correct Doppler scale fairly close.

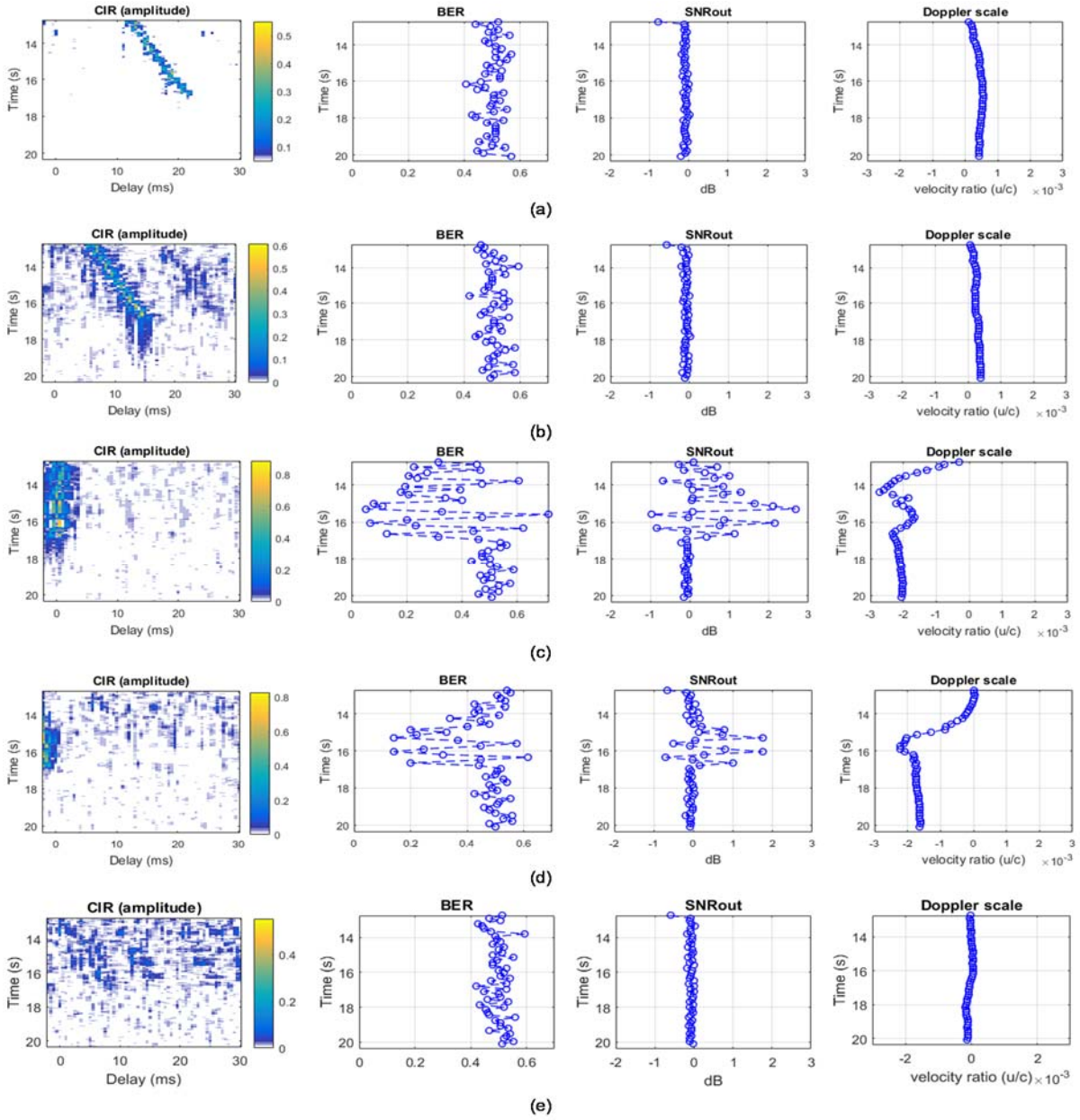

Fig. 4. Performance results for varying signal delays: (a) -12 ms offset. (b) -6 ms offset. (c) perfect delay synchronization. (d) +6 ms offset. (e) +12 ms offset.

4. CONCLUSIONS

In this work, we have presented the application of an adaptive DFE to CAS systems. A 7.7-second, 1000-bps-rate BPSK message was transmitted in the frequency range 1300 - 2500 Hz during the REP-16 Atlantic trials. Our results have shown a high-precision delay/Doppler measurement of echoes moving at a speed of 6 knots in both high and low SNR regimes. The main contribution of this work is that the Doppler measurement update rate of the target is as fast as the bit rate of the transmitted message.

Our results seem promising and pave the way to use more advance equalisation techniques for target tracking. These techniques could be, for example, turbo equalisation or bi-directional DFE and can be extended to 100% duty cycle. Finally, validation of the proposed receiver in operational relevant scenarios under different channel geometries will bring further insights on how suitable this receiver is in real situations.

5. ACKNOWLEDGEMENTS

This work was made possible using data from the REP16-Atlantic sea trial, co-organised by CMRE, the University of Porto, the University of Azores and the Portuguese Navy. Funding was provided by NATO's Allied Command Transformation (ACT).

REFERENCES

[1] **P. C. Hines**, "Experimental comparison of continuous active and pulsed active sonars in littoral waters," In *Proc. 1st International Conference and Exhibition on Underwater Acoustics*, Corfu, Greece, pp. 51-58, 2013.

[2] **P. C. Hines, S. M. Murphy, D. A. Abraham, and G. B. Deane**, "The dependence of signal coherence on sea-surface roughness for high and low duty cycle sonars in a shallow-water channel," *IEEE J. of Ocean. Eng*., vol. 42(2), pp. 298-318, Apr. 2017.

[3] **D. A. Abraham and P. C. Hines**, "Effect of pulse duration on echo matched-filter statistics in a shallow-water channel," *IEEE J. of Ocean. Eng.*, vol. 42(2), pp., 319-334, April 2017.

[4] **R. Plate and D. Grimmett**, "High Duty Cycle (HDC) sonar processing interval and bandwidth effects for the TREX'13 dataset," In *IEEE/MTS OCEANS 2015-Genova*, pp. 1-10, May 2015.

[5] **D. Grimmett and R. Plate**, "Temporal and Doppler coherence limits for the underwater acoustic channel during the LCAS'15 high duty cycle sonar experiment," In *IEEE/MTS OCEANS*-Monterey, pp. 1-9, Sept. 2016.

[6] **L. Jiang, S. Yan, Y. Wu and X. Ma**, "Sonar detection performance with LFM-BPSK combined waveforms," In *OCEANS 2016 - Shanghai*, pp. 1-4, 2016.

[7] **M. G. Meyer and N. A. Rotker**, "Undersea remote sensing with acoustic communications waveforms," In *IEEE/MTS OCEANS 2015-Genova*, pp. 1-6, May 2015.

[8] **K. Pelekanakis and M. Chitre**, "Robust equalization of mobile underwater acoustic channels," *IEEE J. of Ocean. Eng.*, vol. 40, no. 4, pp. 775–784, Oct 2015.

[9] **J. G. Proakis**, *Digital Communications*, 4th ed. McGraw-Hill, 2011.